JCTC Journal of Chemical Theory and Computation

ARTICLE

pubs.acs.org/JCTC

Polarizable Force Fields and Polarizable Continuum Model: A Fluctuating Charges/PCM Approach. 1. Theory and Implementation

Filippo Lipparini* and Vincenzo Barone

Scuola Normale Superiore, Piazza dei Cavalieri 7, 56126 Pisa, Italy

ABSTRACT: We present a combined fluctuating charges−polarizable continuum model approach to describe molecules in solution. Both static and dynamic approaches are discussed: analytical first and second derivatives are shown as well as an extended lagrangian for molecular dynamics simluations. In particular, we use the polarizable continuum model to provide nonperiodic boundary conditions for molecular dynamics simulations of aqueous solutions. The extended lagrangian method is extensively discussed, with specific reference to the fluctuating charge model, from a numerical point of view by means of several examples, and a rationalization of the behavior found is presented. Several prototypical applications are shown, especially regarding solvation of ions and polar molecules in water.

1. INTRODUCTION

The astonishing development of computational resources during recent decades has made possible studies of larger and larger molecular systems together with the computation of accurate and complex physical−chemical properties. Both classical and quantum mechanical (QM) approaches have enormously increased either their range of application or their accuracy or both, allowing the study of several processes ranging from folding studies of huge biological systems to extremely accurate computations of spectroscopic parameters for medium-large molecules.

Complex systems, like nanostructured ones or solutions and, more in general, what is usually referred to as "Soft Matter" represent, nevertheless, an interesting challenge for theoretical and computational chemistry. The huge dimensionality of such systems, which can be considered microscopic but certainly not molecular, is still far beyond the possibilities of modern computational infrastructures: a computational study of a complex system by means of standard tools is nowadays still unfeasible when a QM treatment of the whole system is required. This can be both a curse and a blessing: the quantity of data arising from the direct study of such a system would be difficult to analyze and even more difficult to translate into chemically understandable information when a local property tuned by the chemical environment is the target of the study.

The unfeasibility of "brute force" approaches, on the other hand, is not to be considered as an insuperable obstacle. Chemical intuition is often the way to get a valuable answer at a reasonable price and is the driving force in the definition of *focused models*, where the target of a study is well-defined and distinguished from the environment, as complex as it might be, that surrounds it.

A prototypical focused model may use different levels of theory, from a very sophisticated QM approach to describe the core, to a cheaper one for its closest surroundings, to a classical but still atomistic one for the distant surroundings, to a continuum to describe the boundaries. In this paper, we will focus on the two latter shells and, in particular, on their interface. As the continuum is concerned, the Polarizable Continuum Model (PCM)[1,2] is one of the most successful models, thanks to its generality and its versatility. The PCM represents a solvent, or other more complex matrices[3] such as an anisotropic medium or a weak ionic solution or even a metal nanoparticle, by means of a polarizable, infinite, dielectric medium which surrounds a molecular cavity that accommodates the "solute". However, when dealing with solvents responsible for specific interactions like hydrogen bonds, a continuous approach may not be sufficient to achieve a correct description of the system: a mixed continuous−atomistic treatment of the solvent, using molecular mechanics (MM) to describe the atomistic portion, can be greatly beneficial.[4−12] On the other hand, the mixed strategy is advantageous with respect to a fully atomistic one as the PCM easily takes into account the long-range interactions that would require a huge number of solvent molecules, increasing significantly the computational cost of the simulation, and implcitly includes the statistical average of their configurations.

In this paper, we will present a combined PCM/MM description using a polarizable force field. The most popular approaches used to include polarization effects in MM include the induced point dipole method,[13] the classical Drude oscillator model,[14] and the fluctuating charges model.[15−17]

We find the FQ model particularly appealing in view of its strong connection both with quantum mechanics and classical electrostatics: the model is based on concepts, such as atomic hardness and electronegativity, which can be rigorously defined in the framework of density functional theory (DTF);[18,19] on the other, the electronic distribution is represented by effective atomic charges which interact classicaly. There is a strong connection with the formalism adopted by semiempirical methods, like the density functional tight binding[20,21] approach, and the FQ model, for they both treat the electronic polarization with some suitably defined—and QM derived—charges that are made self-consistent; on the other hand, the same strong formal

Received: June 6, 2011
Published: September 15, 2011

analogy holds between the FQ model and Apparent Surface Charge (ASC) methods like PCM, where the definition of the polarizable charges is classical. We find the smoothness in switching from a classical and continuous description to an atomistic and quantum mechanical one aesthetically fascinating and promising in the perspective of a complete, multiscale description of complex systems. Another advantadge of the FQ model with respect to the point dipole method is that only the electrostatic potential needs to be calculated: as the electric field is discontinuous at the cavity surface, its use can be a source of numerical instabilities which are avoided using only the potential.

Two different possibilities are offered by the FQ model, eventualy coupled with the PCM: It can be used to calculate molecular properties by means of response theory or analytical derivatives in a standard, static fashion or for molecular dynamics simulations. We will refer to the first approach as "time independent" and to the second as "time dependent". In the first case, the FQ model can be used to describe the solute and (or) a few molecules of solvent in a QM/MM/PCM fashion: the standard machinery of computational chemistry can hence be employed to calculate structural and spectroscopic properties.[5,8,12] On the other hand, the PCM is an effective and physically suitable way to enforce nonperiodic boundary conditions (nPBC) in molecular dynamics (MD) simulations.[22−27] While the use of PBC is convenient to describe solids like crystals or metals or pure liquids, this is not always the case when dealing with intrinsically nonperiodic systems, like a molecule in solution: to avoid spurious interactions between the molecule and its copy in a neighboring cell, a large amount of molecules of solvent is to be used. This is especially true with charged solutes, as the Coulomb interaction decays very slowly with the distance.[28−30] The PCM can be successfully and efficiently used to impose boundary conditions by defining a suitable volume (cavity), enclosed by a regular surface like a sphere, a cylinder, or an ellipsoid, that accommodates the solute and the number of molecules of solvent needed to fill the volume. We would like to point out that the PCM treatment of the electrostatics is, in principle, exact: the electrostatic potential is hence well-defined in the whole space, and no discontinuity arises because of the definition of a cavity if this is regular enough.[31] On the other hand, confinement and nonelectrostatic interactions are a more delicate aspect. Nevertheless, it has been shown in the literature[12,26,32−35] that a tailored confinement potential or a proper buffer can provide accurate results also for the description of bulk liquids and avoid compenetrations between the continuous and atomistic portions of the solvent. This is of particular importance when dealing with a polarizable force field, as the penetration of a polarizable molecule in the polarizable dielectric could give rise to instabilities. The aspects of confinement and nonelectrostatics are of course closely related, as the repulsion interaction is responsible for the impossibility for different molecules to compenetrate. The PCM cavity can be kept fixed during the simulation so that the computational cost per step due to the PCM reduces to the calculation of the electrostatic potential at some representative surface point and a matrix/vector multiplication, as will be clarified in section 3. This constraint can be easily relaxed, but while this is necessary in order to do geometry optimizations, previous attempts[22−24] show that a fixed cavity is enough to have a satisfactory description of the solvent.

In this contribution, we will mainly focus on the time dependent approach and hence on molecular dynamics simulations; for the sake of completeness, the FQ contribution to analytical first and second derivatives will be derived in the perspective of a future development in the time independent field of applications. To the best of our knowledge, this is the first derivation of analytical second derivatives for the FQ model.

This paper is organized as follows: In section 2, the FQ model is discussed, and the FQ/PCM equations are derived. Section 3 focuses on analytical derivatives of the FQ/PCM contribution to the energy and on the use of FQ/PCM in molecular dynamics simulations. Finally, in section 4, some preliminary numerical results are presented.

2. THEORY

The FQ model is based on the *electronegativity equalization principle*[18,36] (EEP), which states that, at equilibrium, the instantaneous electronegativity $\tilde{\chi}$ of each atom has the same value. Considering an isolated atom, it is possible to expand in Taylor series its energy with respect to the net charge on the atom itself. To the second order:

$$E = E_0 + \frac{\partial E}{\partial Q} Q + \frac{1}{2} \frac{\partial^2 E}{\partial Q^2} Q^2 \tag{1}$$

The parameters—i.e., the energy derivatives—that appear in eq 1 hold a clear physical significance: the first derivative is in fact a Mulliken electronegativity, while the second is a chemical hardness.

$$\left.\frac{\partial E}{\partial Q}\right|_{Q=0} = \chi, \left.\frac{\partial^2 E}{\partial Q^2}\right|_{Q=0} = 2\eta$$

It is possible to extend eq 1 to a molecular system by taking into account the interaction between charges located on different sites:

$$E = E_0 + \sum_i [\chi_i q_i + \eta_i q_i^2 + \sum_{j>i} J_{ij} q_i q_j] \tag{2}$$

where the hardness kernel **J** represents, as stated, the interaction, and the sum runs over the nuclei. The electronegativity of the *i*th atom is hence defined as the derivative of the energy with respect to the *i*th charge:

$$\tilde{\chi}_i = \frac{\partial E}{\partial q_i} = \chi_i + \sum_j J_{ij} q_j \tag{3}$$

where we put $J_{ii} = 2\eta_i$. The EEP states that the electronegativity of each atom in the molecule has the same value. This can be stated in an equivalent, but more advantageous, formulation defining the atomic partial charges as the constrained minimum of functional

$$F(\mathbf{q}, \lambda) = E_0 + \sum_i [\chi_i q_i + \eta_i q_i^2 + \sum_{j>i} J_{ij} q_i q_j] + \lambda(\sum_i q_i - Q_{tot})$$

where the constraint, imposed by means of a Lagrange multiplier, is meant to preserve the total charge. When more than a molecule is present, there are two possible different strategies to impose the charge constraint:

1. The entire system is constrained to have charge Q_{tot}, and no constraint is imposed on each molecule. This allows

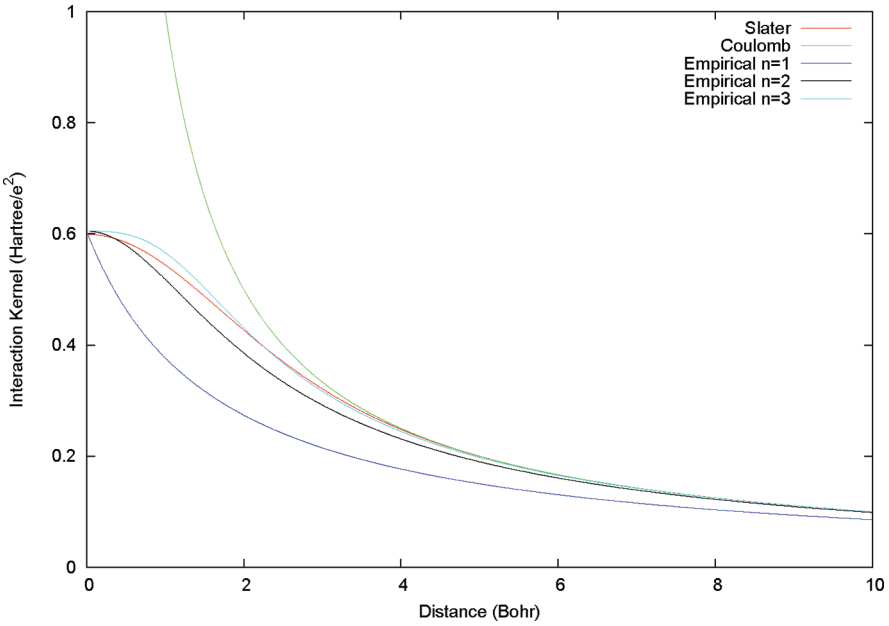

Figure 1. Comparison between different expressions for the interaction kernel.

intermolecular charge transfer and makes, at the equilibrium, the electronegativity of each atom the same.

2. Each molecule is constrained to assume a fixed, total charge Q_α (requiring of course these charges to sum to Q_{tot}). Following this second possibility, the electronegativity of each atom in the same molecule will be the same but will have in general different values among different molecules.

It has been pointed out[15] that the first choice allows for charge transfer even when it is unphysical—i.e., when two molecules are separated by a large distance. In the literature, some models have been proposed[37−42] to take into account in a correct way charge transfer; however, we will not deal with such phenomena here and adopt the second choice for constraints. Dropping the constant term, the functional to be minimized reads thus

$$F(\mathbf{q},\boldsymbol{\lambda}) = \sum_{\alpha,i} q_{\alpha i}\chi_{\alpha i} + \frac{1}{2}\sum_{\alpha,i}\sum_{\beta,j} q_{\alpha i}J_{\alpha i,\beta j}q_{\beta j} + \sum_\alpha \lambda_\alpha \sum_i (q_{\alpha i} - Q_\alpha)$$
$$= \mathbf{q}^\dagger\boldsymbol{\chi} + \frac{1}{2}\mathbf{q}^\dagger\mathbf{J}\mathbf{q} + \boldsymbol{\lambda}^\dagger\mathbf{q} \quad (4)$$

where the Greek indexes run on molecules and the Latin ones on atoms of each molecule.

The interaction kernel **J** describes the Coulomb repulsion between two atoms and, from a quantum mechanical point of view, can be conveniently described in terms of the Coulomb interaction between two charge distributions represented by spherical (s) Slater orbitals:

$$J_{ij}(r_{ij}) = \int_{\mathbb{R}^3} d\mathbf{r}\int_{\mathbb{R}^3} d\mathbf{r}' \frac{|\phi_i(\mathbf{r}-\mathbf{r}_i)|^2|\phi_j(\mathbf{r}'-\mathbf{r}_j)|^2}{|\mathbf{r}-\mathbf{r}'|} \quad (5)$$

where

$$\phi_i(r) = \mathcal{N}_i r^{n_i-1} e^{-\zeta_i r}$$

$\mathcal{N}_i$ is a normalization constant, $\mathbf{r}_i$ is the position of the ith nucleus, n_i is the principal quantum number, and ζ_i is the Slater exponent. This choice was the one proposed by Rappé and co-workers in their pioneering work[36] and is widely pursued in the literature.[15,40,43−46] As the integral in eq 5 goes to the bare coulomb interaction when two sites are sufficiently distant, this choice is usually reserved to the intramolecular terms, while the intermolecular ones are described as classical Coulomb interactions between point charges. This choice is particularly pursued when rigid molecules are considered: the integrals are to be computed only at the beginning of the simulation, and only the intermolecular contributions need to be updated on the fly, which can be done very efficiently using linear scaling techniques. A different, but in principle similar, choice describes the interaction by means of Gaussian orbitals,[19,38,47,48] which allow an easy and efficient computation of the interaction kernel, exploiting the machinery of common quantum chemistry codes. The integrals that need to be calculated are

$$J_{ij}(r_{ij}) = \int_{\mathbb{R}^3} d\mathbf{r}\int_{\mathbb{R}^3} d\mathbf{r}' \frac{|\varphi_i(\mathbf{r}-\mathbf{r}_i)|^2|\varphi_j(\mathbf{r}'-\mathbf{r}_j)|^2}{|\mathbf{r}-\mathbf{r}'|}$$
$$= \frac{1}{r_{ij}}\,\mathrm{erf}\left(\frac{r_{ij}}{\sqrt{R_i^2 + R_j^2}}\right) \quad (6)$$

where

$$\varphi(\mathbf{r}-\mathbf{r}_i) = \frac{1}{(R_i^2\pi)^{3/2}} e^{-\mathbf{r}-\mathbf{r}_i/R_i^2}$$

and R_i is the width of the distribution. Some authors[19,47] generalized the ansatz of s-type functions to s- and p-type Gaussian type orbitals: this allows the model to accurately reproduce out of plane contributions to polarizabilities for planar molecules.

While the use of basis functions is general and elegant, especially when the relation between FQ and the semiempirical model is considered, the computation of the integrals at each step of a molecular dynamics simulation with flexible molecules would be overwhelmingly costly. A different strategy has been

proposed by several authors[49−51] who approximate the Slater integral by means of an empirical Coulombic interaction formula. Let η_{ij} be a parameter related to the interaction of the atoms i and j—for instance, this might be the value of the Slater integral at zero distance, but more in general it can be considered a parameter. The approximate formula is

$$J_{ij}(r_{ij}) = \frac{\eta_{ij}}{[1 + \eta_{ij}^n r_{ij}^n]^{1/n}} \tag{7}$$

In the literature, three different exponents ($n = 1$,[49] $n = 2$,[50] and $n = 3$[51]) have been proposed. We report in Figure 1 the interaction kernel element between an oxygen and a hydrogen atom J_{OH}, as a function of the distance between the two centers, calculated with both eq 5 and eq 7 with the three exponents proposed, in comparison to the bare Coulomb interaction. All of these expressions show the correct asymptotic behavior, and it is possible to see that the approximate formula, eq 7, closely resembles the Slater integral, especially with exponents $n = 2$ and $n = 3$. Throughout this work, we will always adopt the $n = 2$ choice.

The hardness parameters η_{ij} lack a precise physical significance when used to approximate eq 5 but make perfect mathematical sense as the limit for small interatomic distances of the aforementioned integral:

$$\eta_{ij} = \lim_{r_{ij} \to 0} J_{ij}(r_{ij}) \tag{8}$$

As a consequence of their definition, in principle, one should define as many hardness parameters as the number of couples of different atoms. It has been proposed by some authors[50,51] to define the off-diagonal elements as the arithmetical or geometrical averages of the diagonal ones: this is, of course, an approximation, but it reduces greatly the number of parameters to be considered. We will examine the effects of this approximation in section 4 with a numerical example. The obvious advantage of the use of an empirical formula is in terms of computational effort: no integral needs to be evaluated, making the FQ method suitable for flexible molecule MD simulations. This definition of the interaction kernel is the one used in the FQ CharMM force field[52,53] and in the reactive ReaxFF force field.[54]

By taking the derivative of eq 4 with respect to the charges and to the Lagrange multipliers, one obtains the constrained minimum condition:

$$\begin{cases} \sum_{\beta,j} J_{\alpha i,\beta j} q_{\beta j} + \lambda_\alpha = -\chi_{\alpha i} \\ \sum_i q_{\alpha_i} = Q_\alpha \end{cases} \tag{9}$$

This equation can be recast in a more compact formalism introducing the extended **D** matrix:

$$\begin{pmatrix} \mathbf{J} & \mathbf{1}_\lambda \\ \mathbf{1}_\lambda^\dagger & \mathbf{0} \end{pmatrix}$$

where $\mathbf{1}_\lambda$ is a rectangular matrix which accounts for the Lagrangians. The linear system of equation reads now:

$$\mathbf{D}\mathbf{q}_\lambda = -\mathbf{C} \tag{10}$$

where **C** is a vector containing atomic electronegativities and total charge constraints, whereas $\mathbf{q}_\lambda$ is a vector containing charges and Lagrange muiltipliers. It is important to notice that, although **J** is positive definite, **D** is not, so that it is not possible to solve eq 10 by means of standard minimization procedures.

2.1. Coupling the FQ Force Field with the Polarizable Continuum Model. The PCM solves Poisson's equation with suitable boundary conditions in the presence of a dielectric medium with a cavity, where the solute is accommodated. As we are mainly interested in polar solvents involved in hydrogen bond formation, we will restrict our discussion to the conductor-like model (C-PCM);[55−58] a generalization to the IEF-PCM[59−61] model, which we are not concerned about at the moment, is however straightforward. The coupling of a polarizable force field with the PCM requires one to take into account the mutual polarization of the atomistic and continuous part. This problem has recently been solved by Steindal and co-workers[9] in the framework of QM/MM calculation, with the polarization of the force field described by means of Thole's point dipole method.[13] The coupling between the polarizable force field and the PCM is handled by defining the proper extended matrix. We will follow here a slightly different strategy. The recently introduced variational formalism for the PCM[62,63] (V-PCM) recasts the PCM problem in a calculus of variations fashion: the energy of the solvated system is defined as the (unconstrained) minimum of a suitable, strictly convex functional. We report here its expression for the C-PCM (see Appendix ; all of the details can be found in ref 62):

$$\mathcal{G}(\boldsymbol{\sigma}) = \frac{1}{2f(\varepsilon)} \boldsymbol{\sigma}^\dagger \mathbf{S} \sigma + \boldsymbol{\sigma}^\dagger \mathbf{V}[\rho] \tag{11}$$

where $\boldsymbol{\sigma}$ is the vector containing the appearent surface charges that represent the polarization of the dielectric, **S** is the coulomb interaction matrix, **V** is the electrostatic potential produced by the solute *in vacuo*, and ε is the solvent's dielectric permittivity. The scaling factor $f(\varepsilon) = (\varepsilon - 1)/\varepsilon$ is used to adjust the results of the conductor-like model to dielectrics.[56] We point out that an equivalent functional was originally proposed by Klamt and Schuurmann,[55] but it was not fully exploited in its variational aspect.

As discussed in the Introduction, for molecular dynamics related calculations, we will restrict ourselves to fixed cavities surrounded by a regular surface, in particular a sphere, filled with the solute and a suitable number of solvent molecules. This means that the PCM response matrix, which depends only on the geometry of the cavity, can be computed and inverted once for ever at the beginning of the calculation without the need of performing costly linear algebra at each step. It is assumed that the surface of the cavity is partitioned in a suitable mesh and the surface elements are provided with some basis function. The traditional choice[2] is to use piecewise constant functions on the surface elements, which corresponds to reproducing the polarization surface density of charge by means of point charges σ_i. Recently, a new discretization scheme was presented,[64] where the PCM apparent surface charge is expanded in terms of Gaussian functions. This is very convenient when the molecular cavity follows the motion of the solute, as it provides continuous energy and gradients. As in MD simulations, we are only dealing with fixed, regular cavities; we will not adopt the aforementioned scheme both because we would not exploit its advantages and because we are treating the FQ as point charges. A generalization to the continuous surface charge (CSC) formalism of Scalmani and Frisch[64] is straightforward and consistent with the definition of the interaction kernel in terms of the coulomb overlap of

Gaussian orbitals. From the perspective of using the standard PCM cavity to compute molecular properties in a time independent fashion, that is by means of analytical derivatives, the CSC will be necessary to avoid numerical instabilities and discontinuities.

Exploiting the new variational formalism, it is possible to define a (free) energy functional of both the FQ and the PCM polarization charges. We point out that although the PCM free energy functional is strictly convex, this is not the case for the FQ one, as the electroneutrality constraint needs to be imposed; nevertheless, the energy of the coupled system can be written as the constrained minimum of the functional

$$\Lambda(\mathbf{q},\boldsymbol{\sigma},\boldsymbol{\lambda}) = \mathbf{q}^{\dagger}\boldsymbol{\chi} + \frac{1}{2}\mathbf{q}^{\dagger}\mathbf{J}\mathbf{q} + \sum_{\alpha=1}^{NM}\lambda_{\alpha}\sum_{j=1}^{NA}(q_j^{\alpha} - Q_{\mathrm{tot}}^{\alpha}) + \frac{1}{2f(\varepsilon)}\boldsymbol{\sigma}^{\dagger}\mathbf{S}\boldsymbol{\sigma} + \boldsymbol{\sigma}^{\dagger}\Phi(\mathbf{q}) \tag{12}$$

where $\Phi(\mathbf{q})$ is the electrostatic potential due to the FQ at the PCM cavity's surface elements. Let V be the potential due to the PCM charges at the atoms. We can express those potentials in a symmetric fashion as

$$\Phi_i = \sum_{j=1}^{N}\frac{q_j}{|\mathbf{r}_j - \mathbf{s}_i|} \stackrel{\mathrm{def}}{=} \sum_{j=1}^{N}\Omega_{ij}q_j$$
$$V_i = \sum_{j=1}^{\mathrm{NTs}}\frac{\sigma_j}{\mathbf{s}_j - \mathbf{r}_i} = \sum_{j=1}^{\mathrm{NTs}}\Omega_{ij}^{\dagger}\sigma_j$$

where N is the total number of atoms and NTs is the number of PCM surface elements.

These equations define an interaction kernel between the PCM charges and the FQ Ω. Imposing the minimum condition, one has to solve a coupled linear system

$$\begin{pmatrix}\mathbf{D} & \Omega^{\dagger}\\ \Omega & \mathbf{S}/f(\varepsilon)\end{pmatrix}\begin{pmatrix}\mathbf{q}_{\lambda}\\ \boldsymbol{\sigma}\end{pmatrix} = \begin{pmatrix}-\mathbf{C}\\ \mathbf{0}\end{pmatrix} \tag{13}$$

which is consistent with what found by Steindal and co-workers[9] for point dipoles.

It is interesting to spend a few lines on eq 13. As was already pointed out in the Introduction, the EEP leads to a mixed classical/quantum model where the FQs arise from quantum atomic theory but interact in a classical way. On the other hand, PCM is a fully classical model, derived from electrostatics: it describes the polarization response of a classical dielectric medium due to a classical source. From a more formal point of view, the main difference between these two models is that while the fundamental equation of the PCM is Poisson's equation, which relates an electrostatic potential with a classical source, the same does not hold for the FQ model: it is in fact not possible to identify a "source", in the Maxwellian meaning of the term. The source of the FQ is nested in the electronic structure of the system, represented in an approximate fashion by the EEP. These considerations can be extracted by the formal structure of eq 13: the right-hand side of the equation shows a source term for the FQ, the electronegativities, and no external source for the PCM part, which arises from the *classical* density of charge produced by the FQs themselves.

3. ANALYTICAL DERIVATIVES

The gradients of the energy functional are easily derived from eq 4. Differentiating once and using the chain rule:

$$F^{(x_i)}(\mathbf{q},\boldsymbol{\lambda}) = \frac{dF}{dx_i} = \frac{\partial F}{\partial x_i} + \frac{\partial F}{\partial \mathbf{q}}\frac{\partial \mathbf{q}}{\partial x_i} + \frac{\partial F}{\partial \boldsymbol{\lambda}}\frac{\partial \boldsymbol{\lambda}}{\partial x_i}$$

Assuming that eq 10 has been solved, the last two terms vanish; that is, the total derivative and the partial derivative of the functional coincide. This can be seen as a classical equivalent to the Hellman−Feynman theorem for variational methods. Hence:

$$F^{(x_i)}(\mathbf{q},\boldsymbol{\lambda}) = \frac{\partial F(\mathbf{q},\boldsymbol{\lambda})}{\partial r_{ij}}\frac{\partial r_{ij}}{\partial x_i} = \frac{1}{2}\mathbf{q}^{\dagger}\frac{\partial \mathbf{J}}{\partial r_{ij}}\mathbf{q}\frac{x_i}{r_{ij}} \tag{14}$$

In a MMPol-PCM calculation, there is also a contribution arising from the interaction between the FQ and the PCM charges to be added. Following the same arguments, only the partial derivative of eq 12 needs to be calculated:

$$\Lambda^{(x_i)}(\mathbf{q},\boldsymbol{\lambda},\boldsymbol{\sigma}) = \left[\frac{1}{2}\mathbf{q}^{\dagger}\frac{\partial \mathbf{J}}{\partial r_{ij}}\mathbf{q} + \boldsymbol{\sigma}^{\dagger}\frac{\partial \Omega}{\partial r_{ij}}\mathbf{q} + \frac{1}{2f(\varepsilon)}\boldsymbol{\sigma}^{\dagger}\frac{\partial \mathbf{S}}{\partial r_{ij}}\boldsymbol{\sigma}\right]\frac{x_i}{r_{ij}} \tag{15}$$

where, when we work with a fixed cavity, the contribution involving the derivatives of the **S** matrix vanishes.

The second derivatives of eq 4 can be obtained differentiating once again eq 14. Using the chain rule and adopting a more compact notation:

$$F^{(xy)} = \frac{d}{dy}\frac{\partial F}{\partial x} = \frac{\partial^2 F}{\partial x \partial y} + \frac{\partial^2 F}{\partial x \partial \mathbf{q}}\frac{\partial \mathbf{q}}{\partial y} + \frac{\partial^2 F}{\partial x \partial \boldsymbol{\lambda}}\frac{\partial \boldsymbol{\lambda}}{\partial y} \tag{16}$$

the last term of eq 16 vanishes, but it is necessary to compute the derivative of the charges:

$$F^{(xy)} = \frac{1}{2}\mathbf{q}^{\dagger}\mathbf{J}^{(xy)}\mathbf{q} + \mathbf{q}^{\dagger}\mathbf{J}^{(x)}\mathbf{q}^{(y)} \tag{17}$$

Differentiating once eq 10:

$$(\mathbf{D}\mathbf{q}_{\lambda})^{(y)} = \mathbf{D}^{(y)}\mathbf{q}_{\lambda} + \mathbf{D}\mathbf{q}_{\lambda}^{(y)} = 0$$

The derivatives of the charges can thus be obtained solving a *coupled-perturbed* system of equations, which we will call CPFQ in analogy to the coupled-perturbed Hartree−Fock equations:

$$\mathbf{D}\mathbf{q}_{\lambda}^{(y)} = -\mathbf{D}^{(y)}\mathbf{q}_{\lambda} \tag{18}$$

Once again, in a FQ/PCM calculation, the PCM contributions need to be taken into account. A similar set of equations can be obtained differentiating eq 15:

$$\Lambda^{(xy)} = \frac{1}{2}\mathbf{q}^{\dagger}\mathbf{J}^{(xy)}\mathbf{q} + \frac{1}{2f(\varepsilon)}\boldsymbol{\sigma}^{\dagger}\mathbf{S}^{(xy)}\boldsymbol{\sigma} + \boldsymbol{\sigma}^{\dagger}\Omega^{(xy)}\mathbf{q} \tag{19}$$

$$+ \mathbf{q}^{\dagger}\mathbf{J}^{(x)}\mathbf{q}^{(y)} + \boldsymbol{\sigma}^{\dagger}\Omega^{(x)}\mathbf{q}^{(y)} + \mathbf{q}^{\dagger}\Omega^{\dagger(x)}\boldsymbol{\sigma}^{(y)} + \frac{1}{f(\varepsilon)}\boldsymbol{\sigma}^{\dagger}\mathbf{S}^{(x)}\boldsymbol{\sigma}(y) \tag{20}$$

where the derivatives of both the FQ and the PCM charges are obtained solving a set of coupled perturbed equations obtained

differentiating eq 13:

$$\begin{pmatrix} \mathbf{D} & \Omega^{\dagger} \\ \Omega & \mathbf{S}/f(\varepsilon) \end{pmatrix} \begin{pmatrix} \mathbf{q}_{\lambda} \\ \boldsymbol{\sigma} \end{pmatrix}^{(y)} = -\begin{pmatrix} \mathbf{D} & \Omega^{\dagger} \\ \Omega & \mathbf{S}/f(\varepsilon) \end{pmatrix}^{(y)} \begin{pmatrix} \mathbf{q}_{\lambda} \\ \boldsymbol{\sigma} \end{pmatrix} \tag{21}$$

We point out that solving eq 18 or 21 and therefore calculating the derivatives of the FQs gives access to several second order properties, among which are the IR absorption intensities, computed as the derivatives of the dipole moment with respect to the normal modes. Explicit expressions of the first and second derivatives of the interaction kernel are reported in Appendix.

To perform a molecular dynamics simulation, only the energy and its first derivatives are required. Nevertheless, solving eq 10 or 13 at each propagation step would be computationally very demanding; it is however possible to exploit the extended Lagrangian method,[65−68] considering the FQ as independent degrees of freedom endowed with a suitable fictitious mass, like is done in Car−Parrinello[67] MD:

$$\mathscr{L}(\mathbf{R}, \dot{\mathbf{R}}, \mathbf{q}, \dot{\mathbf{q}}) = \frac{1}{2}\mathbf{M}\dot{\mathbf{R}}^2 + \frac{1}{2}\boldsymbol{\mu}\dot{\mathbf{q}}^2 - U(\mathbf{R}) - F(\mathbf{q}, \lambda) \tag{22}$$

The force acting on the ith charge in the αth molecule is obtained differentiating once eq 4 with respect to the charge:

$$\mu\ddot{q}_i^{\alpha} = \frac{\partial F}{\partial \mathbf{q}_{\alpha i}} = -\tilde{\chi}_j^{\alpha} - \lambda_{\alpha} \tag{23}$$

The Lagrangian multipliers can be determined imposing the conservation of the total charge for each molecule, that is:

$$\sum_{i=1}^{\mathrm{NA}} \ddot{q}_i^{\alpha} = 0$$

where NA is the number of atoms in the molecule, and hence

$$\lambda_{\alpha} = -\frac{1}{\mathrm{NA}} \sum_{i=1}^{\mathrm{NA}} \tilde{\chi}_i^{\alpha} \tag{24}$$

Substituting eq 24 into eq 23, one gets

$$\mu\ddot{q}_i^{\alpha} = -\frac{1}{\mathrm{NA}} \sum_{j=1}^{\mathrm{NA}} (\tilde{\chi}_i^{\alpha} - \tilde{\chi}_j^{\alpha}) \tag{25}$$

Equation 25 shows that the dynamics of the charges are governed by the electronegativity equalization principle: the forces that act on the charges arise from differences in the local electronegativities and vanish when the EEP is satisfied.

If a FQ/PCM simulation is done, there is an additional term to be added to the forces on the charge, that is

$$\tilde{\boldsymbol{\chi}} = \mathbf{J}\mathbf{q} + \boldsymbol{\chi} + \mathbf{V} = \mathbf{J}\mathbf{q} + \boldsymbol{\chi} + \Omega\boldsymbol{\sigma} \tag{26}$$

This means that the PCM equations need to be solved to calculate the forces on the charges (and on the nuclei). As we work with a fixed cavity, this can be done easily inverting the PCM matrix separately at the first iteration: the PCM charges can be calculated when necessary, calculating the interaction potential $\boldsymbol{\Phi} = \boldsymbol{\Omega}^{\dagger}\mathbf{q}$ with the FQ and then multiplying it with minus the inverse of the scaled PCM matrix:

$$\boldsymbol{\sigma} = -f(\varepsilon)\mathbf{S}^{-1}\Omega^{\dagger}\mathbf{q}$$

An extended Lagrangian approach for the PCM charges too has been proposed[62,69] and is currently under investigation.

Table 1. Comparison between Analytical and Numerical IR Frequencies (cm^{-1}) and Intensities (km/mol) of NMA

	frequencies		intensities	
mode	analytical	numerical	analytical	numerical
1	88.2116	88.2158	0.0048	0.0049
2	163.5498	163.5521	0.9680	0.9680
3	202.5621	202.5628	0.3784	0.3784
4	303.7496	303.7498	1.4539	1.4539
5	443.8597	443.8598	0.2519	0.2519
6	591.8727	591.8729	2.2844	2.2844
7	635.4398	635.4399	7.8228	7.8230
8	805.8804	805.8805	0.1881	0.1881
9	824.2376	824.2395	86.4033	86.4029
10	965.8140	965.8141	1.5627	1.5627
11	1046.8707	1046.8711	2.0386	2.0386
12	1056.1803	1056.1807	0.3581	0.3581
13	1067.9730	1067.9732	1.9047	1.9047
14	1103.3990	1103.3992	27.8512	27.8511
15	1265.7315	1265.7320	2.5165	2.5165
16	1394.6985	1394.6990	0.0000	0.0000
17	1400.8901	1400.8899	0.2803	0.2803
18	1411.7677	1411.7682	6.6289	6.6289
19	1414.1528	1414.1527	1.7540	1.7540
20	1451.4045	1451.4048	5.7040	5.7040
21	1528.0293	1528.0294	7.6152	7.6152
22	1623.0639	1623.0640	4.3400	4.3400
23	1681.4400	1681.4401	0.0750	0.0750
24	2837.1613	2837.1610	21.5101	21.5101
25	2864.5112	2864.5108	15.3084	15.3084
26	2968.5008	2968.5004	0.1301	0.1301
27	2971.2358	2971.2355	2.5114	2.5114
28	2979.4347	2979.4343	2.6738	2.6738
29	2981.1227	2981.1224	1.3473	1.3473
30	3180.8164	3180.8157	33.2933	33.2934

4. NUMERICAL RESULTS

All of the calculations have been performed with a locally modified development version of the Gaussian[70] suite of programs. As a first numerical test, we report in Table 1 the vibrational frequencies and intensities calculated with eq 17 and by numerical differentiation of the energy gradient for a N-methyl acetamide (NMA) molecule. We employed the AMBER[71] force field endowed with FQs; the electrostatic parameters used for NMA were taken from ref 52 and slightly adjusted to better reproduce the molecule's gas phase dipole moment (see Table 2). We point out that we are not expecting to obtain accurate spectroscopic data, but we are only testing our second derivatives implementation. The discrepancies between the results obtained analytically and numerically are always negligible and reasonably due to the truncation error in numerical differentiation, which is the result we expected. We will not go any further on the time independent approach and focus on the dynamics.

It has been pointed out in the literature[15,42,52] that the time evolution of the extended system defined by the Lagrangian in eq 22 behaves differently whether the molecules are kept rigid or

Table 2. Parameters Used for the NMA/Water Simulations

atoms	χ	η
C	379.83	240.34
H	367.20	501.42
H	367.20	501.42
H	370.10	501.42
C	379.55	214.44
O	430.09	230.06
N	390.88	260.00
H	313.34	517.26
C	380.09	240.34
H	373.02	501.42
H	363.53	501.42
H	373.02	501.42

not. While in the first case little or no thermal coupling is observed between the FQ's dynamics and the atomic one, a strong coupling is observed when intramolecular motions are allowed to take place. To better understand the behavior of the system, we have performed several short simulations with different fictitious masses for the FQs. To avoid as much as possible numerical errors due to the time propagation, we have implemented two very accurate symplectic integrators that, while being very expensive, are known for their long-term stability and accuracy. The time evolution of a classical system can be conveniently described using the Liouville formalism: if $A(\mathbf{q},\mathbf{p})$ is any property of the system that only depends implicitly on time, one has

$$\frac{dA(\mathbf{q},\mathbf{p})}{dt} = \sum_i \left(\dot{q}_i \frac{\partial A}{\partial q_i} + \dot{p}_i \frac{\partial A}{\partial p_i} \right) = \{H, A\}$$

where q_i and p_i are the coordinates and momenta of the particles, H is its Hamiltonian, and $\{\cdot,\cdot\}$ is a Poisson bracket. If one introduces the Liouvillian operator as

$$iLA = \{H, A\}$$

it is possible to write the formal solution of the equations of motion as

$$A(t) = e^{iLt} A(0)$$

Unfortunately, the exponential map cannot be computed explicitly; on the other hand, if we can write

$$iL = iL_T + iL_V$$

that is, if the Hamiltonian is separable into a kinetic and a potential contribution, we have two maps that we know how to explicitly compute. Symplectic integrators approximate the exact time evolution with

$$\exp(i(L_T + L_V)\delta t) \simeq \prod_{j=1}^{k} \exp(ic_j L_T \delta t) \exp(id_j L_V \delta t) + O(\delta t^{k+1}) \quad (27)$$

The order k of the expansion determines the order of the integrator. The first order integrator is also known as the symplectic Euler method, while the second order corresponds to the Verlet method. Following the work of Yoshida,[72] we also implemented a fourth order and a sixth order symplectic integrator, which require respectively three and eight force evaluations per step and are respectively $O(\delta t^5)$ and $O(\delta t^7)$ accurate. We report the coefficients c_i and d_i obtained by Yoshida in his paper in Table 3.

Table 3. Coefficients for the Symplectic Integrator

order	c_i	d_i
2	1/2	1
	1/2	0
4	$1/(2(2-2^{1/3}))$	$1/(2-2^{1/3})$
	$(1-2^{1/3})/(2(2-2^{1/3}))$	$2^{1/3}/(2-2^{1/3})$
	c_2	d_1
	c_1	0
6	0.78451361047756	0.39225680523978
	0.23557321335936	0.51004341191846
	−1.1776799841789	−0.47105338540976
	1.31518632038390	0.068753168252520
	c_3	d_4
	c_2	d_3
	c_1	d_2
	0	d_1

In Figure 2, we report the total energy and the temperature of the charges during the propagation for the first picosecond of a simulation. The propagation was obtained using the fourth order symplectic integrator with a 0.1 fs time step. The test system used is a cluster of 171 water molecules, described with the AMBER-(TIP3P)[71,73] (flexible) force field endowed with fluctuating charges. The parameters used to define the FQ part of the force field are η_O = 367.0 kcal/mol^2, η_H = 392.2 kcal/mol^2, and χ_{OH} = 130.0 kcal/mol. The first two parameters are those given in ref 15, while the electronegativity difference between oxygen and hydrogen has been adjusted to reproduce the dipole moment of liquid water. An extensive and thorough work of parametrization will be the object of a future communication.

We notice that, as the fictitious mass of the FQ is increased, a more intense thermal coupling between the nuclear and FQ dynamics occurs: while with a very small mass (below 50 atomic units) there is almost no coupling and the FQ temperature remains stable around a few degrees Kelvin, it increases rapidly, reaching values near 300−400 K when a bigger mass is used. The same simulation was also carried out without the PCM embedding; we do not report the results, as no significant difference is seen. The behavior of the energy conservation and of temperature fluctuations stabilize and remain mostly unchanged after the first picosecond of simulation.

To be sure that the thermal coupling is not (at least, not only) due to numerical errors during the integration of the equations of motion, we repeated these tests also with the sixth order symplectic integrator: the results are reported in Figure 3

We notice that, in any simulation, the energy drifts are always very small (below 0.1 kcal/mol) and almost not noticeable (below 3×10^{-5} kcal/mol) when using the sixth order integrator; nevertheless, the thermal coupling is always strong when the FQ fictitious mass is above 50 atomic units.

These results seem to suggest that a small mass has to be used in order to avoid an excessive energy transfer from the nuclei to the charges; on the other hand, a small mass limits the propagation to a very small time step. We report in Figure 4 the energy conservation for a fictitious mass of 25 au and 150 au for different

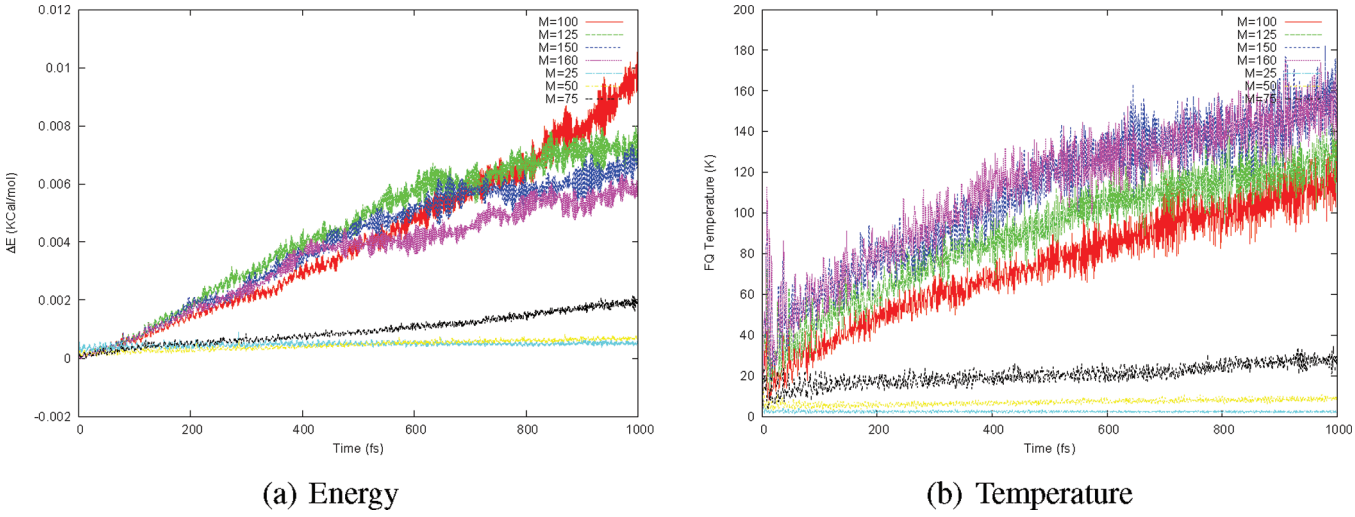

Figure 2. Energy conservation and temperature of the FQ with different fictitious masses for the FQ−fourth order integrator.

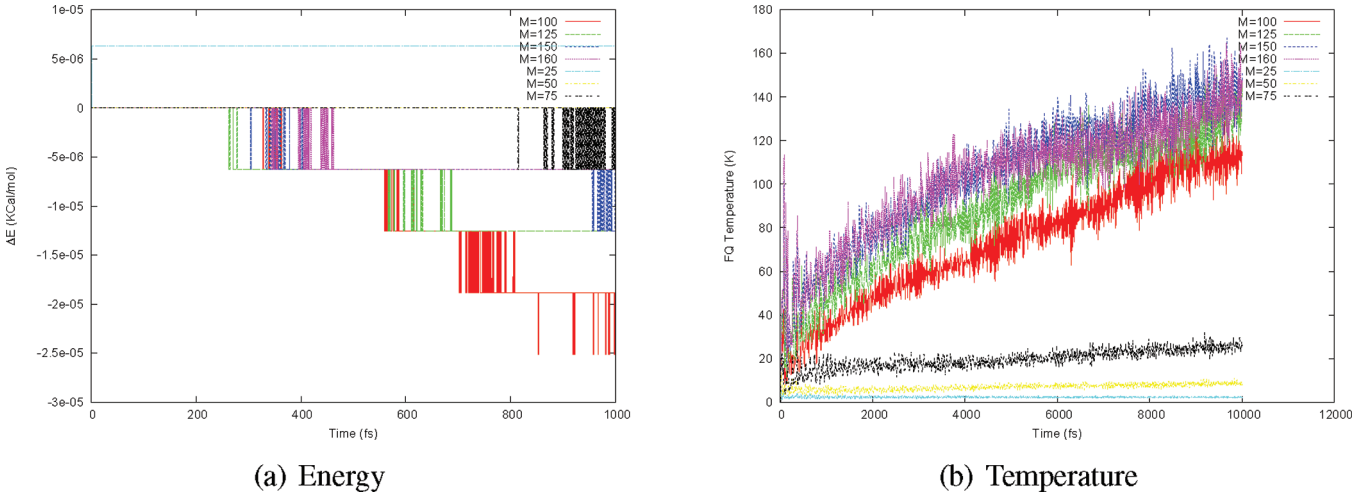

Figure 3. Energy conservation and temperature of the FQ with different fictitious masses for the FQ−sixth order integrator.

time steps. With the smaller mass, the propagation could not be carried out with a time step longer than 0.25 fs, while it remained reasonably stable even with a 0.4−0.5 fs time step when using the heavier mass.

To overcome this difficulty,[15,52] the thermal coupling can be removed by thermostatting separately the nuclei and the charges at two different temperatures. This allows one to propagate the system using a large fictitious mass for the charges and hence a reasonable time step. Nevertheless, the time step chosen to propagate the charges cannot be too small if molecules are not kept rigid, as the polarization energy should be considered a "fast" motion: the order of magnitude of its variation with respect to the molecular geometry is comparable to that of the bonding energy terms in a force field. This is shown in Figure 5, where the O−H stretching energy is compared with the electrostatic energy as a function of the O−H distance.

This behavior can be rationalized by considering the motion of the FQs at a fixed geometry. Following the elegant analysis of Olano and Rick,[46] it is possible to calculate a frequency of oscillation for some suitably defined linear combination of the charges, considered dynamical variables. Following Olano and Rick, let us consider an isolated molecule of water at its equilibrium geometry (C_{2v} symmetry). Imposing explicitly the constraint on the total charge, i.e.

$$q_O = -2q_H$$

where the hydrogens carry the same charge for symmetry reasons, the electrostatic energy reads:

$$U(q_H) = \frac{1}{2}\begin{pmatrix} q_{H1} \\ q_{H2} \end{pmatrix}^{\dagger} \begin{pmatrix} \alpha & \beta \\ \beta & \alpha \end{pmatrix} \begin{pmatrix} q_{H1} \\ q_{H2} \end{pmatrix} + \Delta\boldsymbol{\chi}\dagger\mathbf{q} \qquad (28)$$

where

$$\Delta\chi_i = \chi_i - \chi_O, \alpha = J_{HH}(0) + J_{OO}(0) - 2J_{OH}(r_{OH}),$$
$$\beta = J_{HH}(r_{HH}) + J_{OO}(0) - 2J_{OH}(r_{OH})$$

The eigenvalues of this matrix correspond, when divided by the charge fictitious mass, to the oscillation frequency of the charge "normal modes". With our values, the eigenvalues are $\lambda_1 = 0.4298$ au, corresponding to a "symmetric" oscillation, and 0.31378 au, corresponding to an asymmetric one. In Figure 6, we report the

dx.doi.org/10.1021/ct200376z |J. Chem. Theory Comput. 2011, 7, 3711–3724

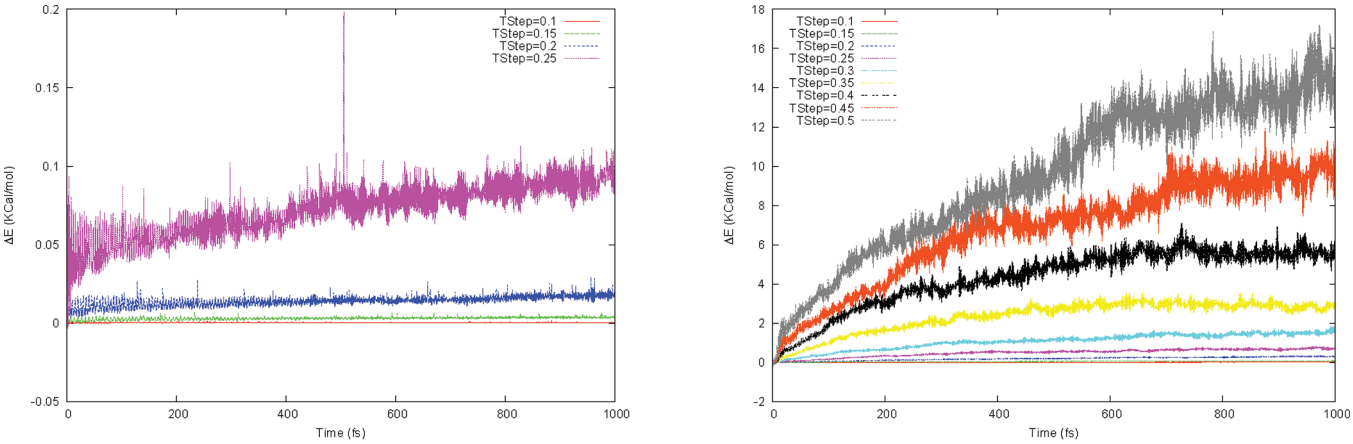

Figure 4. Energy conservation with different FQ fictitious masses and time steps.

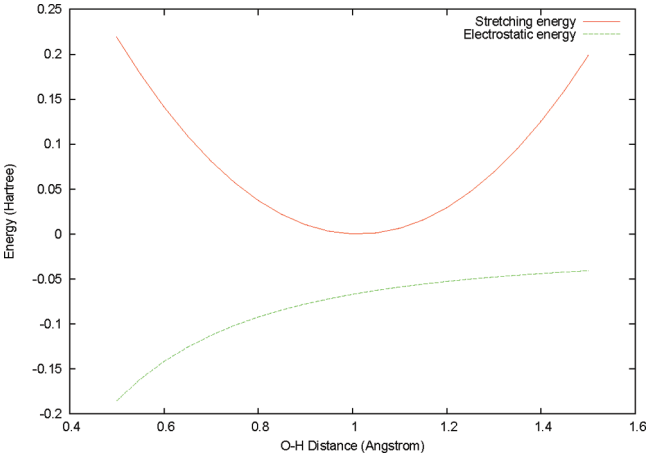

Figure 5. Stretching and electrostatic energy with respect to O−H distance.

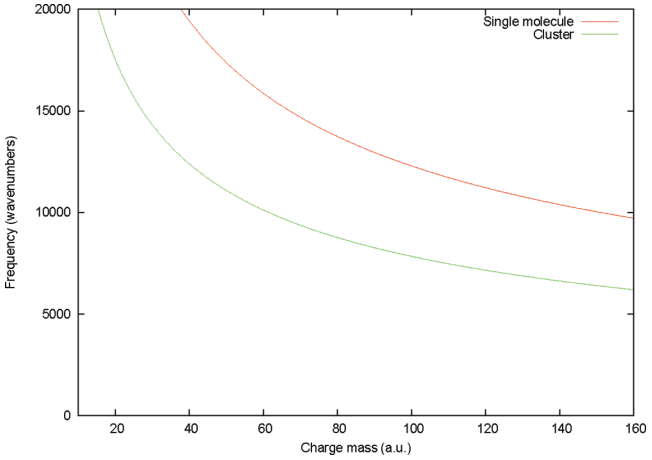

Figure 6. Oscillation frequency for the lowest energy charge normal mode as a function of the fictitious mass for a single molecule of water and for a cluster of water molecules.

frequency as a function of the fictitious mass for the lowest eigenvalue. We see that, while no value of the fictitious mass makes the frequency close to a typical vibrational frequency (which could cause a resonance and, hence, a numerical catastrophe), with large values of the fictitious mass, the separation becomes smaller. On the other hand, small masses correspond to very high characteristic frequencies, hence the necessity of using a very small time step. If we consider a system of interacting molecules, the analysis becomes trickier. Without performing a detailed and accurate treatment of the problem in terms of normal modes, it is possible to estimate the frequency of the lowest energy vibration by the lowest eigenvalue of the **J** matrix. We report in the same Figure 6 the results for the cluster containing 171 molecules that we used for the tests reported at the beginning of this section. Although the numbers are not quantitatively accurate, they certainly provide a qualitatively correct picture of the dynamics of the charges. When the biggest mass is used, the oscillation frequency of the lowest energy normal mode is relatively close to an O−H stretching: this explains the strong thermal coupling between the polarization and atomic degrees of freedom.

To test our implementation, we tried to reproduce the first peak of the pair correlation function for water. A 100 ps simulation was performed at 298 K and unitary density, using the velocity Verlet integrator, with a 0.25 fs time step. The system was composed of 457 molecules of water in a spherical box of radius r_c = 14.5 Å. The starting configuration was obtained with a standard (N,V,T) simulation at 298 K.

When enforcing nPBCs, spurious boundary effects can occur, which should be cured employing either effective potentials or proper buffer regions.[12,26,32−35] In the present study, we have employed a simple radial potential V_c, which is sufficient for the description of local effects far from the boundaries. More reliable effective potentials will be implemented after the optimization of polarizable flexible solvent force fields. In particular, we adopt for the V_c potential a sixth-degree polynomial expression:

$$V_c(r) = \begin{cases} 0 & r \le r_c \\ k(r - r_c)^6 & r > r_c \end{cases}$$

The temperature was kept constant using a stochastic Andersen

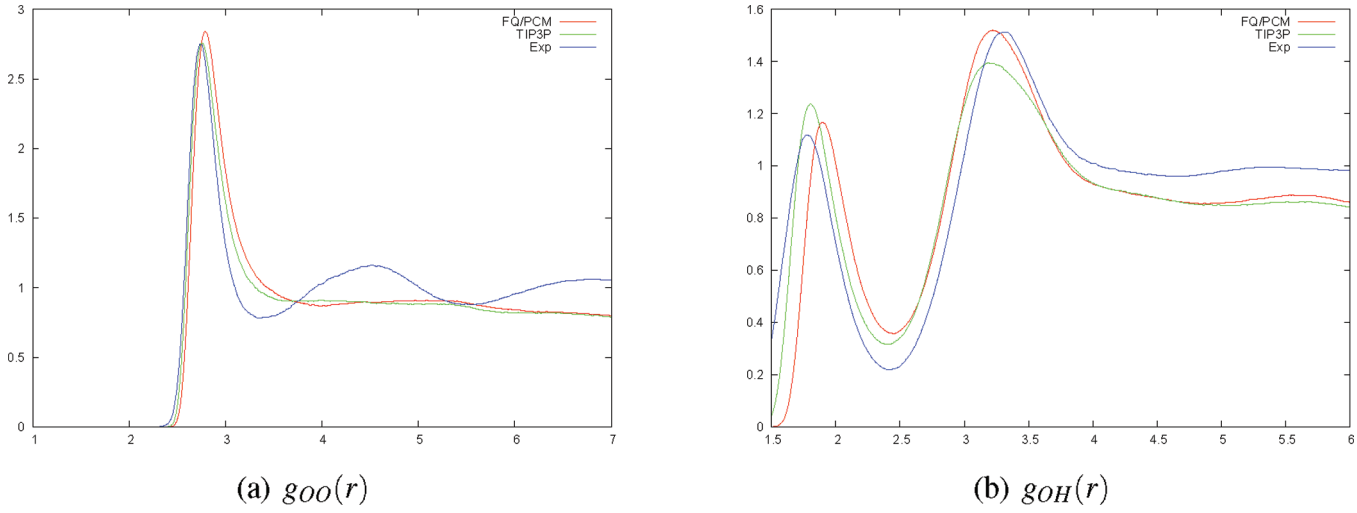

Figure 7. O−O and O−H (intermolecular) radial distribution function for water.

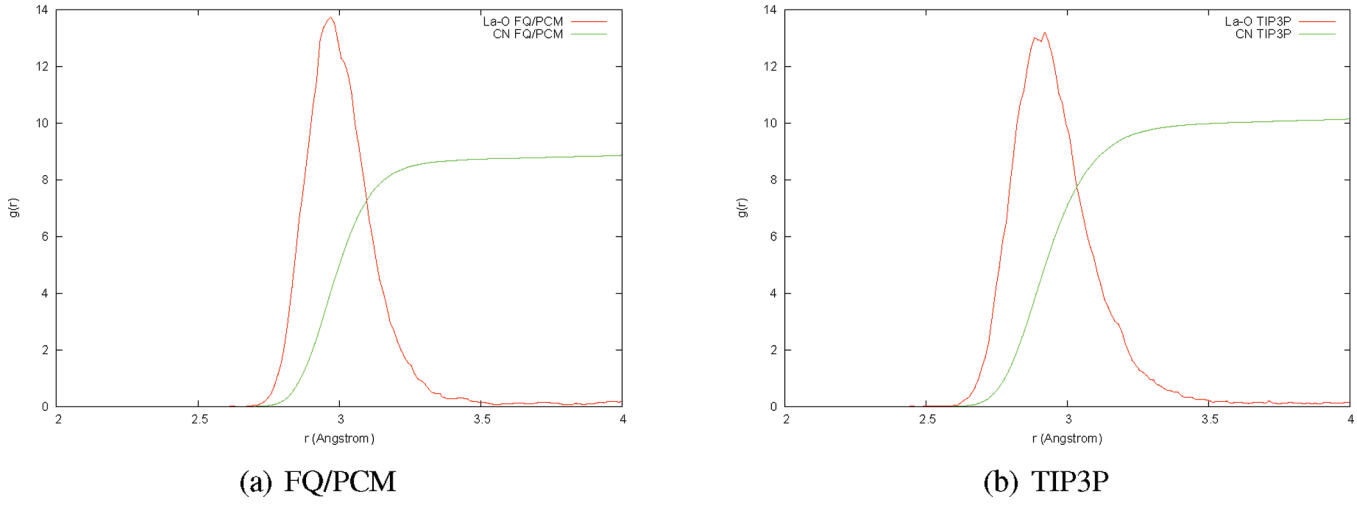

Figure 8. First peak of the La−O radial distribution function and its integral (coordination number).

thermostat[65] for the nuclei and rescaling the velocities for the charges so that their temperature remained fixed to 4 K. We used the AMBER/TIP3P[71,73] force field for the nonelectrostatic part of the potential energy. The system was surrounded by a PCM spherical cavity of radius 15.5 Å. We used a larger radius for the PCM cavity to avoid contact between the FQ and the PCM apparent surface charge and, hence, the potential polarization catastrophe. The simple potential adopted was able to enforce the confinement, allowing a very small penetration of the $r > r_c$ region. The size of the PCM cavity with respect to the confinement radius will be the object of further study.

In Figure 7, we report the radial distribution function we obtained with a FQ/PCM simulation and a nonpolarizable TIP3P simulation in comparison to the experimental one of Soper and Phillips.[74] A simulation carried out with 1116 molecules of water confined in a 20.5 Å sphere surrounded by a PCM spherical cavity of radius 21.5 Å produced comparable results. The agreement is only qualitatively acceptable; on the other hand, since a thorough parametrization was not carried out, as regards either the force field or the confinement potential, we did not expect to perfectly reproduce the properties of the bulk liquid.

On the other hand, we felt that the agreement was satisfactory enough to try to reproduce the solvation properties of a cation like lanthanum. It was shown by Duvail and co-workers[75,76] that a polarizable force field is necessary to correctly describe the coordination of lanthanides in water. We hence tried to reproduce their results, adopting the same Buckingham-6 potential they propose to describe the nonelectrostatic interaction of the cation with the solvent and our FQ force field. A 100 ps simulation was carried out on in a 12.5 Å spherical box, obtained cutting the cluster used for the water simulation, and creating a hollow, 3 Å in radius cavity in the middle that accommodates a lanthanum ion, surrounded by 241 water molecules. A 0.25 fs time step and the velocity Verlet integrator were employed. The system was thermostatted at 298 K (4 K for the FQ as before), and data were collected after a 2 ps of equilibration, as suggested by Duvail and co-workers.[75] Confinement was kept as before with a sixth degree polynomial potential, and the system was surrounded with a 13.5 Å spherical PCM cavity. The La−O radial

distribution function was calculated and the coordination number determined as the area of the first peak. We report in Figure 8 the first peak of the $g_{La-O}(r)$ function and its integral obtained with the FQ polarizable force field and PCM embedding in comparison to the ones obtained with the TIP3P force field. The FQ/PCM calculation gives a coordination number for the La^{3+} ion of slightly less than 9 (8.78), which is in good agreement with both the result obtained by Duvail et al. and the experimental data they report. On the other hand, the unpolarizable force field gives a coordination number slightly bigger than 10 (10.1), again in agreement with what Duvail and co-worker observed.

As a last pilot application of the method implemented, we studied the solvation of a N-methyl acetamide (NMA) molecule in water. The starting configuration was obtained as for the lanthanum ion, cutting a 12.5 Å sphere of water molecules from the cluster used for the pure water simulation and creating a 3 Å cavity to accommodate the NMA molecule. The system was equilibrated for 2 ps, and a 100 ps simulation was run with a 0.25 fs time step, using the velocity Verlet integrator. We employed the AMBER[71,73] force field (TIP3P for water) endowed with fluctuating charges. The FQ parameters were take from ref 52; we slightly adjusted the electronegativities to better reproduce the NMA's gas phase dipole moment (see Table 2). Confinement was maintained with the same sextic potential, and a 13.5 Å PCM cavity surrounded the system. We report in Figure 9 the dipole moment of the NMA molecule along the simulation and in Figure 10 the radial distribution function between the NMA carbonyl oxygen and water and between the NMA amide hydrogen and water, respectively. The results obtained are consistent with those of Patel and co-workers,[52] which was to be expected, as we used a only slightly modified version of their parameters. The radial distribution functions show the presence of a strong hydrogen bond between NMA and water. As Patel and co-workers have already pointed out, the dipole moment of the NMA molecule in water is higher (the average is slightly lower than 8 D) than the one obtained by *ab initio* computation, with implicit or explicit solvation (5.18 to 5.33 D). In our case, this overpolarization effect can be attributed to two different facts. As we have already pointed out, this work was not concerned with the parametrization of a FQ polarizable force field: we used parameters taken from the literature, eventually making some adjustment, but without a thorough effort to produce a general and reliable set of parameters. On the other hand, we think that one of the assumptions made is probably a considerable source of error. The definition of the off-diagonal elements of the hardness matrix in eq 8 is an approximation, and

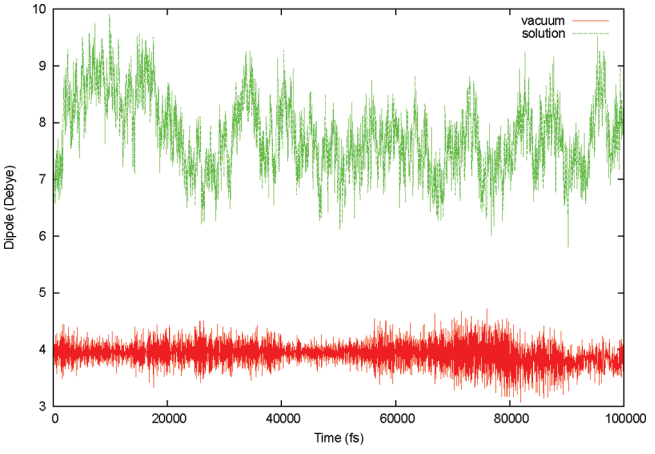

Figure 9. Istantaneous dipole moment (Debye) of the NMA molecule in solution during the simulation.

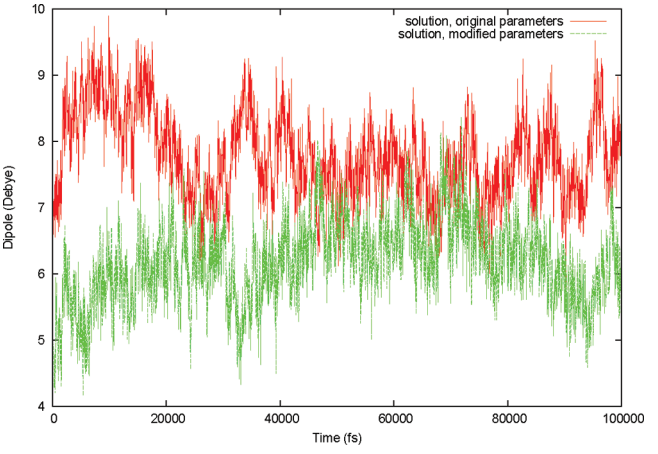

Figure 11. Istantaneous dipole moment (Debye) of the NMA molecule in solution during the simulation—original vs modified parameters.

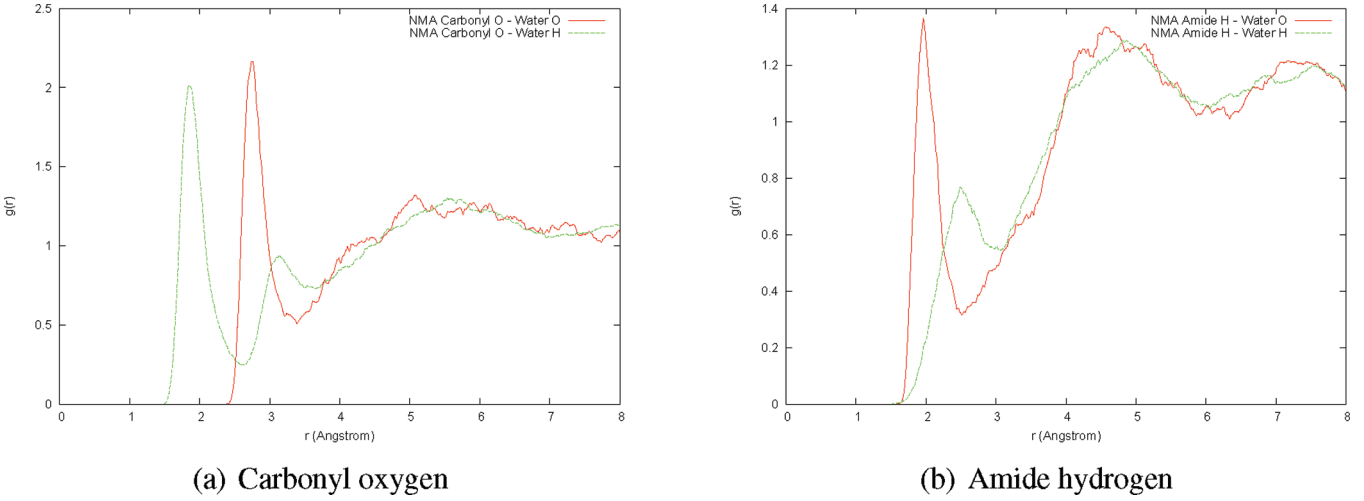

Figure 10. Radial distribution functions for NMA's hydrogen bond donors/acceptors and water's atoms.

dx.doi.org/10.1021/ct200376z |*J. Chem. Theory Comput.* 2011, 7, 3711–3724

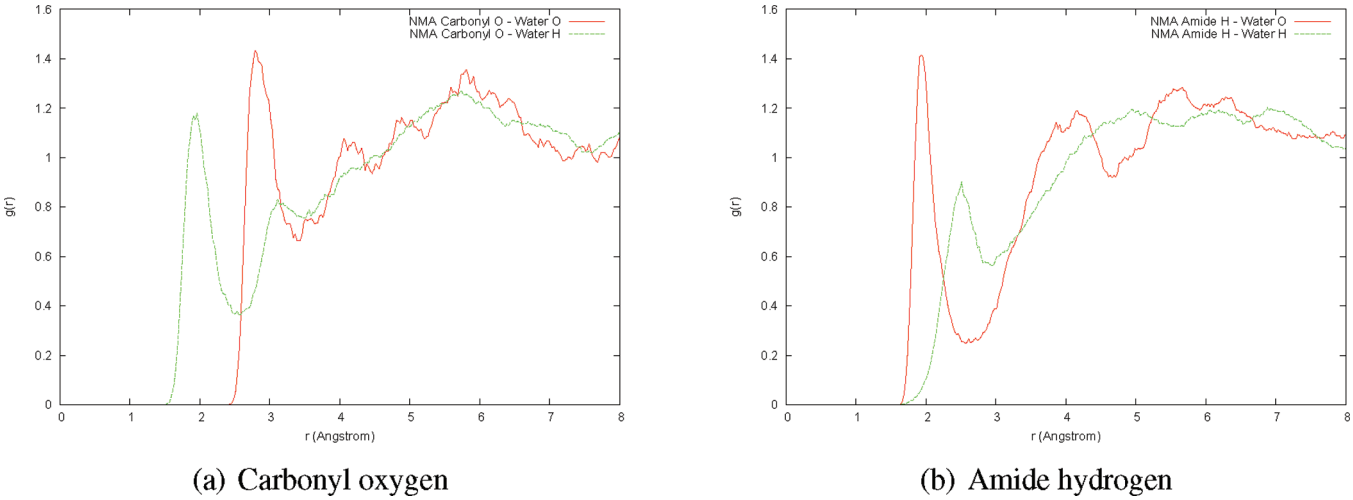

Figure 12. Radial distribution functions for NMA's hydrogen bond donors/acceptors and water's atoms with modified parameters.

we feel it to be a little too simplistic, especially when strong, specific interactions are involved. As a matter of fact, the whole model does not consider covalent or "quantum" interactions at all: when dealing with hydrogen bonds, it is probably necessary to add some degrees of freedom in the parametrization. To show this, we run a simulation changing the off diagonal hardness elements for the atoms involved in hydrogen bond formation, i.e., the amide hydrogen with the water oxygen and the carbonyl oxygen with the water hydrogen. We lowered the values obtained as the arithmetical mean of the atomic ones from $\eta_{H_{NMA}O_{wat}}$ = 311.14 kcal/mol to $\eta_{H_{NMA}O_{wat}}$ = 300.00 kcal/mol and from $\eta_{H_{NMA}O_{wat}}$ = 442.20 kcal/mol to $\eta_{H_{NMA}O_{wat}}$ = 420.00 kcal/mol. We reiterate that this is only a conceptual experiment and that an accurate determination of the optimal parameters has not yet been done. The results are reported in Figures 11 and 12. We see that with the modified parameters, the instantaneous dipole moment oscillates around a value (slightly larger than 6.0 D) which is much closer to the one obtained by *ab initio* calculations; on the other hand, the simulation provides a much weaker formation of hydrogen bonds, as shown by the heights of the peaks in Figure 12. A small extension of the manifold of parameters hence seems definitely worth the effort.

5. CONCLUSIONS AND PERSPECTIVES

We have implemented a polarizable force field using the fluctuating charges model, and we have combined it with the polarizable continuum model as a tool to perform molecular dynamics simulations with nonperiodic boundary conditions in NVE/NVT ensembles. Extensive numerical testing has been performed to better understand the behavior of the MD simulations when the charges are propagated in a Car–Parrinello-like fashion, and a rationalization has been proposed on the basis of the analysis of the frequencies of oscillation that characterize the charge dynamics. Several prototypical applications have been shown: calculation of IR frequencies and intensities and simulation of pure water and of charged and uncharged atomic and molecular solutes have been performed and discussed. We notice that the lack of an accurate parametrization of the whole force field is probably the first problem that needs to be addressed. From the NMA simulations, we found that the manifold of parameters that need to be taken into account for the electrostatics can have a crucial effect on the quality of the results: its extension with parameters chosen to describe specific intermolecular interactions might introduce major improvements. As pointed out by Verstraelen and coworkers[41] in their excellent work, parametrization is a complex matter, and the literature presents sets of parameters widely varying in one respect to another, all because the cost functions used for calibration present flat and elongated minima. Another important extension of the model that we have not considered yet is charge transfer.[15,40,43−46] It has been shown that this phenomenon can be of great importance in determining the properties of liquid water, in which, as we aim to model aqueous solutions, we are very interested. Concerning more specifically molecular dynamics, other ensembles, especially the NPT one,[77] need to be considered, and a more exhaustive study on the effect of different thermostats is under investigation. In particular, the use of the Andersen barostat combined with Nosé−Hoover−Poincaré thermostats may be convenient, as it allows the propagation of the trajectory with an arbitrary order symplectic integrator. The perspectives of a FQ/PCM implementation are many. The FQ model provides the electrostatic interactions to the ReaxFF reactive force field:[54] reactivity in solution by means of classical MD simulations is an interesting development. On the other hand, an interface with the QM world seems the most promising target to pursue, especially considering that our implementation is rooted in a very QM-oriented computational package. From this point of view, the FQ polarizable force field is the missing term in the GLOB[22−26] model, where the core and the continuum are polarizable but the atomistic layer of the solvent is not. A fully polarizable QM/MM/PCM layered method, suitable both for accurately reproducing the solvent effect on molecular properties and for mixed classical/ab initio molecular dynamics, is, after the aforementioned developments are complete, an important target we wish to pursue.

APPENDIX A. THE C-PCM AS A VARIATIONAL PROBLEM

The conductor-like PCM describes the solvent as a conducting medium which occupies all the space but a hollow cavity that accommodates the solute. Let C be such cavity, which we will assume to be a bounded, simply connected open subset of $\mathbb{R}^3$

with regular enough boundary $\Gamma = \partial C$, and let ρ be the molecular density of charge, which we will assume to be supported inside C. As we are assuming that the cavity is surrounded by a conductur, the potential at the boundary must vanish, and hence we need to solve the Poisson equation

$$\nabla^2\phi = -4\pi\rho, \phi = 0 \ \forall \ \mathbf{r} \notin C \tag{29}$$

Linearity allows us to write the potential as a sum of a molecular term Φ and a reaction term V_r, due to the polarization of the surroundings:

$$\phi = \Phi + V_r$$

The molecular term is the potential produced by the density ρ *in vacuo*, while the reaction term can be modeled as the potential produced by an apparent surface charge σ, which represents the polarization of the medium:

$$\Phi(\mathbf{r}) = \int_C \frac{\rho(\mathbf{r}')}{|\mathbf{r}-\mathbf{r}'|}\,d\mathbf{r}', V_r(\mathbf{r}) = \int_\Gamma \frac{\sigma(\mathbf{s})}{|\mathbf{r}-\mathbf{s}|}\,d\mathbf{s}$$

As the total potential must vanish at the boundary, the C-PCM integral equation will read:

$$V_r(\mathbf{s}) = \int_\Gamma \frac{\sigma(\mathbf{s}')}{|\mathbf{s}-\mathbf{s}'|}\,d\mathbf{s}' \stackrel{\text{def}}{=} (\mathcal{S}\sigma)(\mathbf{s}) = -\Phi(\mathbf{s}) \tag{30}$$

where we have introduced the integral operator $\mathcal{S}$. It is known[31] that if Γ is regular enough, $\mathcal{S}$ is a self-adjoint, positive definite, coercive operator in a suitable Hilbert space V: this means that the (unique) minimum of the functional

$$J(\sigma) = \frac{1}{2}\langle\sigma, \mathcal{S}\sigma\rangle_V + \langle\sigma, \Phi|_\Gamma\rangle_V \tag{31}$$

(we denote with $\langle\cdot,\cdot\rangle_V$ the scalar product in V) is also the solution of the integral equation.[78] Adding the C-PCM scaling factor $1/(f(\varepsilon))$ and discretizing, eq 11 is recovered.

APPENDIX B. DERIVATIVES OF THE FQ CONTRIBUTION TO THE ENERGY: EXPLICIT CONTRIBUTIONS

During the calculation of the gradients and of the Hessian of the FQ contribution to the energy, both first and second partial derivatives of the interaction kernel eq 7 are to be computed. We report here their expressions.

$$\frac{\partial J_{ij}}{\partial r_k^\mu} = (1-\delta_{ij})\frac{\partial J_{ij}}{\partial r_{ij}}\frac{r_i^\mu - r_j^\mu}{r_{ij}}(\delta_{ik}-\delta_{jk}) \tag{32}$$

where r_k^μ is the μth Cartesian coordinate of the position vector of the kth particle and

$$r_{ij}^2 = \sum_{\mu=1}^{3}(r_i^\mu - r_j^\mu)^2 = \sum_{\mu=1}^{3}(r_{ij}^\mu)^2$$

We will need to calculate

$$\frac{\partial J_{ij}}{\partial r_{ij}} = \frac{\partial}{\partial r_{ij}}\frac{\eta_{ij}}{(1+r_{ij}^n\eta_{ij}^n)^{1/n}} = -\frac{\eta_{ij}^{n+1}r_{ij}^{n-1}}{(1+\eta_{ij}^n r_{ij}^n)^{1/n+1}} \tag{33}$$

In particular, if we choose $n = 2$, eq 32 becomes

$$\frac{\partial J_{ij}}{\partial r_i^\mu} = -\frac{\eta_{ij}^3 r_{ij}^\mu}{(1+\eta_{ij}^2 r_{ij}^2)^{3/2}} \tag{34}$$

The partial second derivative has a rather cumbersome expression:

$$\frac{\partial^2 J_{ij}}{\partial r_k^\mu \partial r_l^\nu} = \frac{\partial^2 J_{ij}}{\partial r_{ij}^2}\frac{\partial r_{ij}}{\partial r_k^\mu}\frac{\partial r_{ij}}{\partial r_l^\nu} + \frac{\partial J_{ij}}{\partial r_{ij}}\frac{\partial^2 r_{ij}}{\partial r_k^\mu \partial r_l^\nu} \tag{35}$$

The second derivative of the interaction kernel with respect to the interatomic distance is

$$\frac{\partial^2 J_{ij}}{\partial r_i^\mu \partial r_j^\nu} = \frac{\eta_{ij}^{n+1}r_{ij}^{n-2}(2r_{ij}^n\eta_{ij}^n - n + 1)}{(1+\eta_{ij}^n r_{ij}^n)^{1/n+2}}$$

With our $n = 2$ choice, eq 35 becomes

$$\frac{\partial^2 J_{ij}}{\partial r_k^\mu \partial r_l^\nu} = (1-\delta_{ij})\left\{\frac{3\eta_{ij}^5 r_{ij}^\mu r_{ij}^\nu}{(1+\eta_{ij}^2 r_{ij}^2)^{5/2}} - \delta_{\mu\nu}\frac{\eta_{ij}^3}{(1+\eta_{ij}^2 r_{ij}^2)^{3/2}}\right\}$$
$$[\delta_{kl}(\delta_{ik}+\delta_{jk}) - (1-\delta_{kl})(\delta_{ik}\delta_{jl}+\delta_{il}\delta_{jk})] \tag{36}$$

AUTHOR INFORMATION

Corresponding Author
*E-mail: f.lipparini@sns.it.

ACKNOWLEDGMENT

The authors gratefully acknowledge financial support from Gaussian, Inc.

REFERENCES

(1) Tomasi, J.; Persico, M. *Chem. Rev.* **1994**, *94*, 2027–2094.
(2) Tomasi, J.; Mennucci, B.; Cammi, R. *Chem. Rev.* **2005**, *105*, 2999–3093.
(3) Mennucci, B. *J. Phys. Chem. Lett.* **2010**, *1*, 1666–1674 and references therein.
(4) Vreven, T.; Mennucci, B.; da Silva, C.; Morokuma, K.; Tomasi, J. *J. Chem. Phys.* **2001**, *115*, 62–72.
(5) Rega, N.; Cossi, M.; Barone, V. *J. Am. Chem. Soc.* **1998**, *120*, 5723–5732.
(6) Cui, Q. *J. Chem. Phys.* **2002**, *117*, 4720–4728.
(7) Pedone, A.; Biczysko, M.; Barone, V. *ChemPhysChem* **2010**, *11*, 1812–1832.
(8) Barone, V.; Bloino, J.; Monti, S.; Pedone, A.; Prampolini, G. *Phys. Chem. Chem. Phys.* **2010**, *12*, 10550–10561.
(9) Steindal, A. H.; Ruud, K.; Frediani, L.; Aidas, K.; Kongsted, J. *J. Phys. Chem. B* **2011**, *115*, 3027–3037.
(10) Rega, N.; Cossi, M.; Barone, V. *J. Am. Chem. Soc.* **1997**, *119*, 12962–12967.
(11) Benzi, C.; Improta, R.; Scalmani, G.; Barone, V. *J. Comput. Chem.* **2002**, *23*, 341–350.
(12) Barone, V.; Biczysko, M.; Brancato, G. Extending the Range of Computational Spectroscopy by QM/MM Approaches: Time-Dependent and Time-Independent Routes. In *Combining Quantum Mechanics and Molecular Mechanics. Some Recent Progresses in QM/MM Methods*; Sabin, J. R., Canuto, S., Eds.; Academic Press: Waltham, MA, 2010; Vol. 59, pp 17 − 57.
(13) Thole, B. *Chem. Phys.* **1981**, *59*, 341–350.
(14) Lamoureux, G.; Roux, B. *J. Chem. Phys.* **2003**, *119*, 3025–3039.
(15) Rick, S. W.; Stuart, S. J.; Berne, B. J. *J. Chem. Phys.* **1994**, *101*, 6141–6156.
(16) Rick, S. W.; Berne, B. J. *J. Am. Chem. Soc.* **1996**, *118*, 672–679.
(17) Rick, S. W.; Stuart, S. J.; Bader, J. S.; Berne, B. J. *J. Mol. Liq.* **1995**, *65−66*, 31–40.

(18) Mortier, W. J.; Van Genechten, K.; Gasteiger, J. *J. Am. Chem. Soc.* **1985**, *107*, 829–835.
(19) Chelli, R.; Procacci, P. *J. Chem. Phys.* **2002**, *117*, 9175–9189.
(20) Elstner, M.; Porezag, D.; Jungnickel, G.; Elsner, J.; Haugk, M.; Frauenheim, T.; Suhai, S.; Seifert, G. *Phys. Rev. B* **1998**, *58*, 7260–7268.
(21) Trani, F.; Barone, V. *J. Chem. Theory Comput.* **2011**, *7*, 713–719.
(22) Brancato, G.; Rega, N.; Barone, V. *J. Chem. Phys.* **2006**, *124*, 214505.
(23) Brancato, G.; Nola, A. D.; Barone, V.; Amadei, A. *J. Chem. Phys.* **2005**, *122*, 154109.
(24) Rega, N.; Brancato, G.; Barone, V. *Chem. Phys. Lett.* **2006**, *422*, 367–371.
(25) Brancato, G.; Barone, V.; Rega, N. *Theor. Chem. Acc.* **2007**, *117*, 1001–1015.
(26) Brancato, G.; Rega, N.; Barone, V. *J. Chem. Phys.* **2008**, *128*, 144501.
(27) Rega, N.; Brancato, G.; Petrone, A.; Caruso, P.; Barone, V. *J. Chem. Phys.* **2011**, *134*, 074504.
(28) Smith, P. E.; Pettitt, B. M. *J. Chem. Phys.* **1996**, *105*, 4289–4293.
(29) Hünenberger, P. H.; McCammon, J. A. *J. Chem. Phys.* **1999**, *110*, 1856–1872.
(30) Bergdorf, M.; Peter, C.; Hünenberger, P. H. *J. Chem. Phys.* **2003**, *119*, 9129–9144.
(31) Cancès, E. In *Continuum Solvation Models in Chemical Physics*; Mennucci, B., Cammi, R., Eds.; Wiley: New York, 2007.
(32) Warshel, A.; King, G. *Chem. Phys. Lett.* **1985**, *121*, 124–129.
(33) King, G.; Warshel, A. *J. Chem. Phys.* **1989**, *91*, 3647–3661.
(34) Luzhkov, V.; Warshel, A. *J. Comput. Chem.* **1992**, *13*, 199–213.
(35) Sham, Y. Y.; Warshel, A. *J. Chem. Phys.* **1998**, *109*, 7940–7944.
(36) Rappe, A.; Goddard, W. *J. Phys. Chem.* **1991**, *95*, 3358–3363.
(37) Chen, J.; Martinez, T. J. *Chem. Phys. Lett.* **2008**, *463*, 288.
(38) Chelli, R.; Pagliai, M.; Procacci, P.; Cardini, G.; Schettino, V. *J. Chem. Phys.* **2005**, *122*, 074504.
(39) Nistor, R. A.; Polihronov, J. G.; Müser, M. H.; Mosey, N. J. *J. Chem. Phys.* **2006**, *125*, 094108.
(40) Lee, A. J.; Rick, S. W. *J. Chem. Phys.* **2011**, *134*, 184507.
(41) Verstraelen, T.; Bultinck, P.; Van Speybroeck, V.; Ayers, P. W.; Van Neck, D.; Waroquier, M. *J. Chem. Theory Comput.* **2011**, *7*, 1750–1764.
(42) Ando, K. *J. Chem. Phys.* **2001**, *115*, 5228–5237.
(43) Chelli, R.; Ciabatti, S.; Cardini, G.; Righini, R.; Procacci, P. *J. Chem. Phys.* **1999**, *111*, 4218–4229.
(44) Llanta, E.; Ando, K.; Rey, R. *J. Phys. Chem. B* **2001**, *105*, 7783–7791.
(45) Llanta, E.; Rey, R. *Chem. Phys. Lett.* **2001**, *340*, 173–178.
(46) Olano, L. R.; Rick, S. W. *J. Comput. Chem.* **2005**, *26*, 699–707.
(47) York, D. M.; Yang, W. *J. Chem. Phys.* **1996**, *104*, 159–172.
(48) Verstraelen, T.; Speybroeck, V. V.; Waroquier, M. *J. Chem. Phys.* **2009**, *131*, 044127.
(49) Nishimoto, K.; Mataga, N. *Z. Phys. Chem. (Frankfurt)* **1957**, *12*, 335.
(50) Ohno, K. *Theor. Chem. Acc.* **1964**, *2*, 219–227.
(51) Louwen, J. N.; Vogt, E. T. C. *J. Mol. Catal. A* **1998**, *134*, 63–77.
(52) Patel, S.; Brooks, C. *J. Comput. Chem.* **2004**, *25*, 1–15.
(53) Patel, S.; Mackerell, A.; Brooks, C. *J. Comput. Chem.* **2004**, *25*, 1504–1514.
(54) van Duin, A. C. T.; Dasgupta, S.; Lorant, F.; Goddard, W. A. *J. Phys. Chem. A* **2001**, *105*, 9396–9409.
(55) Klamt, A.; Schuurmann, G. *J. Chem. Soc., Perk. Trans. 2* **1993**, 799–805.
(56) Barone, V.; Cossi, M. *J. Phys. Chem. A* **1998**, *102*, 1995–2001.
(57) Cossi, M.; Rega, N.; Scalmani, G.; Barone, V. *J. Comput. Chem.* **2003**, *24*, 669–681.
(58) Scalmani, G.; Barone, V.; Kudin, K.; Pomelli, C.; Scuseria, G.; Frisch, M. *Theor. Chem. Acc.* **2004**, *111*, 90–100.
(59) Cancès, E.; Mennucci, B.; Tomasi, J. *J. Chem. Phys.* **1997**, *107*, 3032–3041.
(60) Cancès, E.; Mennucci, B. *J. Math. Chem.* **1998**, *23*, 309–326.
(61) Mennucci, B.; Cancès, E.; Tomasi, J. *J. Phys. Chem. B* **1997**, *101*, 10506–10517.
(62) Lipparini, F.; Scalmani, G.; Mennucci, B.; Cancès, E.; Caricato, M.; Frisch, M. J. *J. Chem. Phys.* **2010**, *133*, 014106.
(63) Lipparini, F.; Scalmani, G.; Mennucci, B.; Frisch, M. J. *J. Chem. Theory Comput.* **2011**, *7*, 610–617.
(64) Scalmani, G.; Frisch, M. J. *J. Chem. Phys.* **2010**, *132*, 114110.
(65) Andersen, H. C. *J. Chem. Phys.* **1980**, *72*, 2384–2393.
(66) Parrinello, M.; Rahman, A. *Phys. Rev. Lett.* **1980**, *45*, 1196–1199.
(67) Car, R.; Parrinello, M. *Phys. Rev. Lett.* **1985**, *55*, 2471–2474.
(68) Crescenzi, O.; Pavone, M.; De Angelis, F.; Barone, V. *J. Phys. Chem. B* **2005**, *109*, 445−453, PMID: 16851035.
(69) Caricato, M.; Scalmani, G.; Frisch, M. J. In *Continuum Solvation Models in Chemical Physics*; Mennucci, B., Cammi, R., Eds.; Wiley: New York, 2007.
(70) Frisch, M. J.; Trucks, G. W.; Schlegel, H. B.; Scuseria, G. E.; Robb, M. A.; Cheeseman, J. R.; Scalmani, G.; Barone, V.; Mennucci, B.; Petersson, G. A.; Nakatsuji, H.; Caricato, M.; Li, X.; Hratchian, H. P.; Izmaylov, A. F.; Bloino, J.; Zheng, G.; Sonnenberg, J. L.; Hada, M.; Ehara, M.; Toyota, K.; Fukuda, R.; Hasegawa, J.; Ishida, M.; Nakajima, T.; Honda, Y.; Kitao, O.; Nakai, H.; Vreven, T.; Montgomery, J. A., Jr.; Peralta, J. E.; Ogliaro, F.; Bearpark, M.; Heyd, J. J.; Brothers, E.; Kudin, K. N.; Staroverov, V. N.; Kobayashi, R.; Normand, J.; Raghavachari, K.; Rendell, A.; Burant, J. C.; Iyengar, S. S.; Tomasi, J.; Cossi, M.; Rega, N.; Millam, J. M.; Klene, M.; Knox, J. E.; Cross, J. B.; Bakken, V.; Adamo, C.; Jaramillo, J.; Gomperts, R.; Stratmann, R. E.; Yazyev, O.; Austin, A. J.; Cammi, R.; Pomelli, C.; Ochterski, J. W.; Martin, R. L.; Morokuma, K.; Zakrzewski, V. G.; Voth, G. A.; Salvador, P.; Dannenberg, J. J.; Dapprich, S.; Daniels, A. D.; Farkas, Ö.; Foresman, J. B.; Ortiz, J. V.; Cioslowski, J.; Fox, D. J. *Gaussian Development Version*, Revision H.10; Gaussian Inc.: Wallingford, CT, 2010.
(71) Cornell, W.; Cieplak, P.; Bayly, C.; Gould, I.; Merz, K.; Ferguson, D.; Spellmeyer, D.; Fox, T.; Caldwell, J.; Kollman, P. *J. Am. Chem. Soc.* **1995**, *117*, 5179–5197.
(72) Yoshida, H. *Phys. Lett. A* **1990**, *150*, 262–268.
(73) Jorgensen, W. L.; Chandrasekhar, J.; Madura, J. D.; Impey, R. W.; Klein, M. L. *J. Chem. Phys.* **1983**, *79*, 926–935.
(74) Soper, A. K.; Phillips, M. G. *Chem. Phys.* **1986**, *107*, 47–60.
(75) Duvail, M.; Souaille, M.; Spezia, R.; Cartailler, T.; Vitorge, P. *J. Chem. Phys.* **2007**, *127*, 034503.
(76) Duvail, M.; Vitorge, P.; Spezia, R. *J. Chem. Phys.* **2009**, *130*, 104501.
(77) Brancato, G.; Rega, N.; Barone, V. *Chem. Phys. Lett.* **2009**, *483*, 177–181.
(78) Ern, A.; Guermond, J.-L. *Theory and Practice of Finite Elements*; Springer: Berlin, 2004; Vol. 159, pp 81−84.